MECHANICS OF GRANULAR MATERIALS AT LOW EFFECTIVE STRESSES

By Stein Sture,[1] Member, ASCE, Nicholas C. Costes,[2] Fellow, ASCE, Susan N. Batiste,[3] Student Member, ASCE, Mark R. Lankton,[4] Khalid A. AlShibli,[5] Associate Member, ASCE, Boris Jeremic,[6] Associate Member, ASCE, Roy A. Swanson,[7] and Melissa Frank,[8] Student Member, ASCE

ABSTRACT: Six displacement-controlled, conventional, drained axisymmetric triaxial experiments on cohesionless granular soil specimens were conducted at very low effective confining stresses in a SPACEHAB module on the Space Shuttle during the STS-79 and STS-89 missions. Three specimens were tested on each mission. The specimens measured 75 mm in diameter by 150 mm long. The average grain size of the subangular Ottawa quartz sand was 0.22 mm. The specimens' relative density for the STS-79 mission was 86.5% (±0.8%); for the STS-89 mission it was 65.0% (±1.0%). The confining stresses in the six experiments were 0.05, 0.52, and 1.30 kPa. Very high friction angles in the range of 47.6 to 70.0° were observed. The dilatancy angles were also unusually high, in the range of 30 to 31°. In spite of the very low effective stresses, high elastic moduli were observed.

INTRODUCTION

Unlike materials such as metals, polymers, and cementitious composites such as concrete, rocks, etc., the strength and deformation characteristics of which are mainly derived from strong cohesive forces from chemical cementation, the constitutive and stability behavior of uncemented granular materials such as sand, which include strength, dilatancy, stiffness modulus behavior, localization of deformation, and shear band formation, are to a large extent derived from the fabric or geometry of the grain structure and interparticle friction resulting from normal forces acting on particles or particle groups. Particle bonding by weak electrostatics and short- or long-range Coulombic forces may also play a role to a certain extent; however, the main source of the constitutive and stability properties of cohesionless granular materials is interparticle friction, which in turn under low confinement stress levels is strongly affected by gravitational body forces under terrestrial (1 gravity) conditions. Costes and Sture (1981), Bolton (1986), Jaeger and Nagel (1996, 1997), and Jaeger et al. (1996) provide detailed reviews of the behavior of granular materials.

The force-displacement behavior of granular materials is highly nonlinear, dilatant, and nonconservative. The gravity-induced stresses in terrestrial laboratory specimens are nearly of the same order of magnitude as the externally applied tractions, thus limiting the size of the specimens. On the other hand, the same laboratory specimens must be sufficiently large to be statistically representative and replicate the behavior of large geologic deposits in situ or the behavior of large masses of industrial products during storage, handling, and transportation. In terms of size effect, it appears that the smallest dimension in a specimen should at least be 100 times larger than the average grain diameter (Sture et al. 1988). For most naturally occurring geologic deposits adequate laboratory specimens should have sizes larger than 50 mm.

Under moderate-to-high stress levels, the influence of gravity on the behavior of experiments may not be pronounced and therefore the test results in a terrestrial environment may be acceptable for engineering purposes. However, the conduct of experiments on granular materials under very low stress levels and under quasi-static conditions can only be performed in a microgravity environment (Costes and Sture 1981). During critical, unstable states, such as liquefaction of saturated loose sands during earthquakes and wave loading, landslides due to pore water pressure buildup, or the collapse of sensitive clays, gravity acts as a follower load, thus making it difficult to study such phenomena in the laboratory or in the field (Scholz 1990). It should be emphasized again that the laboratory specimen that on one hand should resemble a magnified version of the elemental cube in a mechanics sense, should on the other hand be representative of the real mass particle fabric. The gravity-induced stresses within the specimen transform the experiment into a complex boundary value problem, where the constitutive properties and material stability issues cannot be resolved by inverse identification techniques due to the highly nonlinear nature of the constitutive and stability behavior (Sture et al. 1988). In view of these constraints the microgravity environment of space provides the ideal setting for studying the behavior of cohesionless materials at low stress levels in the absence of body forces, and where also the boundary conditions are carefully controlled.

EXPERIMENTS

A series of displacement-controlled cyclic triaxial compression experiments were performed in a SPACEHAB module on the Space Shuttle during the STS-79 mission to Mir in September 1996 and the STS-89 mission in January 1998. The experiments were conducted on six right cylindrical specimens 75 mm in diameter and 150 mm long at effective confining pressures of 0.05, 0.52, and 1.30 kPa. The displacement-controlled experiment configuration was chosen in order to maintain overall specimen-apparatus stability in the event strain-softening phenomena were significant or deformations were to be localized in narrow shear bands, which often lead to overall loss of stability and brittleness phenomena. Displacements were controlled through stiff, highly polished tungsten carbide

[1]Prof. and Chair, Dept. of Civ., Envir. and Arch. Engrg., Univ. of Colorado, Campus Box 428, Boulder, CO 80309. E-mail: sture@grieg.colorado.edu.

[2]Sr. Sci., Space Sci. Lab., Marshall Space Flight Ctr., Huntsville, AL 35812.

[3]Res. Asst., Dept. of Civ., Envir. and Arch. Engrg., Univ. of Colorado, Campus Box 428, Boulder, CO.

[4]Program Mgr., Lab. for Atmospheric and Space Phys., Univ. of Colorado, Campus Box 590, Boulder, CO.

[5]Res. Assoc., Univ. of Colorado, Marshall Space Flight Ctr., Huntsville, AL.

[6]Asst. Prof., Dept. of Civ. and Envir. Engrg., Clarkson Univ., Potsdam, NY 13699-5710.

[7]Res. Assoc., Univ. of Colorado, Marshall Space Flight Ctr., Huntsville, AL.

[8]Res. Asst., Marshall Space Flight Ctr., Huntsville, AL.

Note. Discussion open until December 1, 1998. To extend the closing date one month, a written request must be filed with the ASCE Manager of Journals. The manuscript for this paper was submitted for review and possible publication on February 18, 1998. This paper is part of the ***Journal of Aerospace Engineering***, Vol. 11, No. 3, July, 1998. ©ASCE, ISSN 0893-1321/98/0003-0067–0072/$8.00 + $.50 per page. Paper No. 17717.

end-platens intended to provide very low friction (4.5°) at the end-platen to specimen interface. A constant confining pressure was transmitted through a highly flexible, thin, latex rubber membrane surrounding the cylindrical surface between the end-platens. In each experiment, five axial compression, unloading, and reloading cycles were completed at regular intervals. Data were recorded in detail in all three experiments, including axial load, axial displacement, confining pressure, bulk volumetric changes, confining pressure, and ambient temperature and acceleration levels. Video cameras and a recorder provided 360° coverage of the specimens and monitored overall behavior to track the onset of formation of shear bands or other forms of instability. A regular grid was printed on the specimens' membrane surfaces, which facilitated tracking of motion throughout the conduct of each test. After the experiments were performed, the specimens were epoxy-impregnated and subjected to nondestructive X-ray computed tomography. At a later stage the specimens will be saw cut into sections for further study of pore space distribution, internal fabric features, and zones of instability.

The specimens, which were tested in the dry condition, consisted of subangular quartz (Ottawa) sand with average grain size of 0.22 mm. The Ottawa sand was pretumbled and particles finer than No. 200 US Sieve (0.074 mm) were removed. The specimens were prepared in a terrestrial laboratory by slow pluviation (raining) of the dry sand into a natural rubber latex membrane having a thickness of 0.30 mm, supported by a removable cylindrical mold to ensure uniform density at 86.5% (±0.8%) relative density for the STS-79 mission and 65.0% (±1.0%) for the STS-89 mission, based on a maximum porosity of 0.446, minimum porosity of 0.327, and specific density of the particles of 2.65. The ends of the cylindrical specimens were then sealed by the tungsten carbide end-platens. A small amount of vacuum, which was typically in the range of 13 to 35 kPa relative to the outside atmospheric pressure, was applied through one end-platen to the pore space within each specimen. Measurements of the specimen verified that no significant compaction took place during application of this and subsequently higher confining pressures. The specimen preparation mold was then disassembled and removed. The external test cell was then assembled around the specimen, filled with deionized water, and pressurized to 103.5 kPa. The internal vacuum was then removed and the pore space was vented to atmospheric pressure. Measurements showed that the specimens did not change in density or shape during the application of the isotropic confining pressure. The homogeneity of the specimens' densities was determined with a specially designed penetrometer on ground test specimens prepared by identical procedure, and by X-ray computed tomography techniques on the flight specimens.

Diffusion of water through the membrane into the pore space of the specimen was insignificant. The fluid conductivity of the latex membrane was 10^{-12} m/s. Ground-based long-duration experiments conducted at the same confining pressure (103.5 kPa) showed that on the average 1.60 g of water were transmitted to the specimen over a period of six months. The flight specimens were actually stored for a period of less than three months prior to flight. In view of these considerations, the moisture content was less than 0.7% and no measurable capillary forces were observed. While significant electrostatic forces often are generated during pluviation of dry sand, it was established that the electrostatic forces were discharged

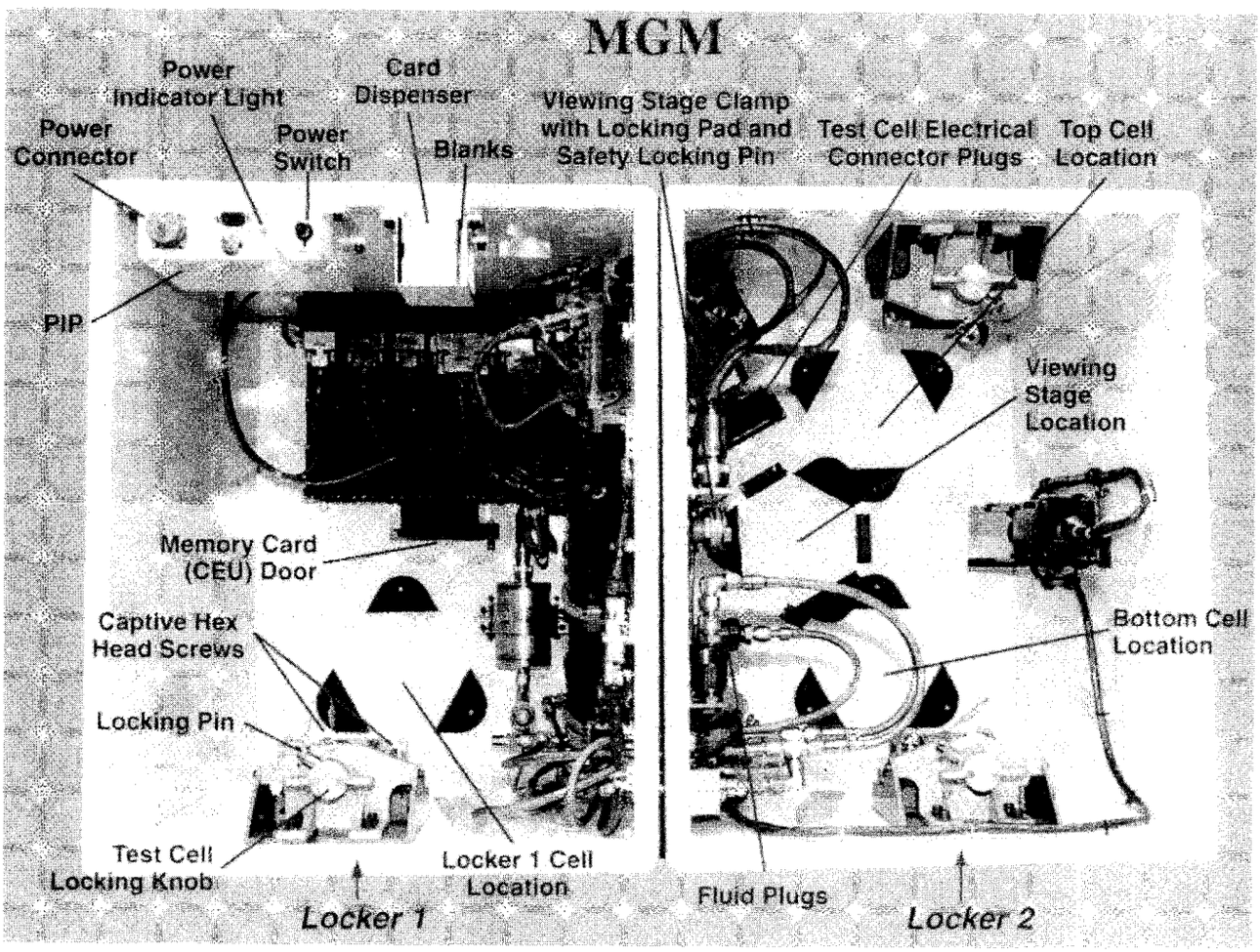

FIG. 1. Twin Double Locker Assembly with Control Electronics, Fluid Accumulators and Lines, and Mounting Points for Test Cells

soon after deposition and the electrostatic effects were negligible at the time the experiments were conducted.

In the following discussions the three experiments (0.05, 0.52, and 1.30 kPa; 85% relative density) conducted on STS-79 will be referred to as the F1 tests, while the three experiments (0.05, 0.52, and 1.30 kPa; 65% relative density) conducted on STS-89 will be referred to as the F2 tests.

EXPERIMENTAL APPARATUS

The experiment hardware for each of the two sets of flight experiments consisted of a control apparatus and three test cells. The control apparatus was contained in a twin double locker assembly (Fig. 1) located on the forward bulkhead of the SPACEHAB module. It provided microprocessor control of the experiments including pressure control of the specimen pore space and the confining fluid, displacement control, and data recording. It also provided mounting points for three test cells during ascent and descent, a viewing stage where test cells were mounted during experiments, and three video cameras located around the viewing stage to provide 360° coverage of the specimen. Pressure accumulators set and maintained the effective confining pressure applied to the membrane-specimen surface, by controlling both the specimen internal (air) and external (water) pressures. The confining pressure was in all three experiments controlled within a range of ±0.03 kPa. Volume change was measured by overall movement of the cell (water) accumulator; displacement was measured by the movement of the test cell loading ram. Both of these were driven by stepper motors, and the record of steps taken by the motors was converted into distance. Load was measured by an internal load cell, with ±310-N range.

The test cells which contained the specimen were quite different from a conventional cylindrical axisymmetric triaxial apparatus. Fig. 2 shows one of the flight test cells. The main body of the test cell had the shape of an equilateral triangular prism, with a transparent Lexan water jacket held between aluminum top and bottom plates. Three internal tension rods tied these parts together and also provided linear bearing surfaces for the upper loading plate, which compressed the specimen. The top and bottom plates of the test cell contained quick connect/disconnect fluid fittings, which allowed pressure control of both the inside of the specimen and the confining fluid (deionized water). The flat faces of the Lexan water jacket allowed minimal distortion of the camera views. Front-lighting of the specimen was provided by light-emitting diode (LED) arrays built into the corners of the Lexan jacket.

The test cell top plate, Lexan jacket, and bottom plate took the place of the traditional load frame. The upper loading plate slid over the three internal tension rods on linear bearings and was driven by a stepper motor/geartrain/screw mounted to the top plate. The nominal displacement rate during loading was 35 mm/h, and the rate during the five unloading-reloading cycles each specimen was reduced to 17.5 mm/h in order to enhance the data recording during the cyclic motion and to enhance system stability. A load cell was directly mounted on the loading plate and connected to the screw by a loading ram. It should be emphasized that the load cell was internal to the cell, and thus did not measure the frictional resistance between the loading ram and sealing o-rings in the top plate as the loading ram entered the test cell, which otherwise would have a very large effect on load cell readings, as overall loads measured are generally less than 70 N. The stationary lower loading plate was built into the bottom plate of the test cell.

The faces of the loading plates were fitted with highly polished tungsten carbide platens, with a measured angle of friction with F-75 Ottawa sand in the range of 4.5°. The two platens were oversized, each having diameters of 95.3 mm, compared to the 75 mm diameter of the specimen. While the intention of the oversized loading platen was to provide room for the specimen to expand during testing, it also hindered free movement of the specimen to a significant extent at the ends due to the stiffness of the stretched latex membrane over the 95.3-to-75-mm-diameter transition, as well as apparently high latex-tungsten adhesion particularly after the prolonged pre-launch storage. Although not generally ideal for a triaxial test, this equipment effect provided additional stabilization of the specimens during launch and landing vibration and accelerations. The radial stress added by the stretched membrane was approximately 2.0 kPa at a radial strain of 20%. The membrane behavior was linearly elastic in this range.

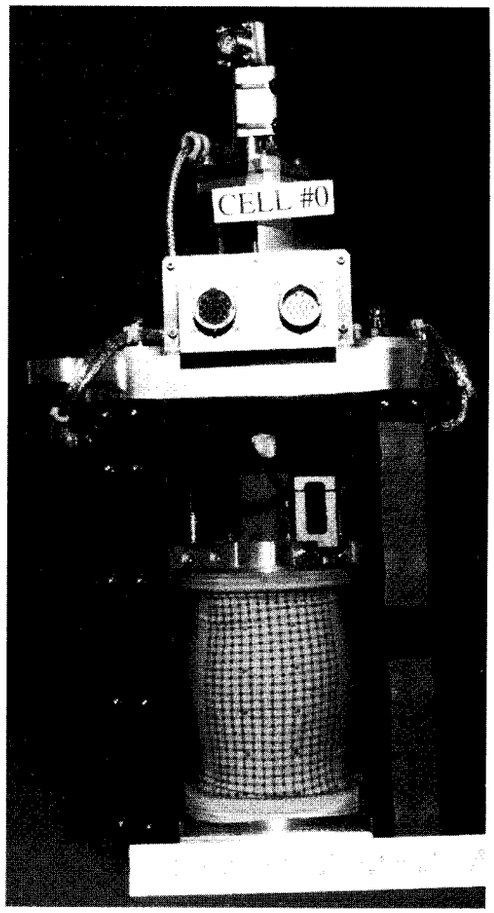

FIG. 2. Test Cell as Seen After Flight. Internally Mounted Load Cell Is Seen on Top of Loading Plate at Top of Specimen. Stepper Motor that Drives Loading Ram Is at Top of Assembly. Vertical Black Covers on Corners of Test Cell Cover LED Bars that Illuminate Specimen

EXPERIMENTAL RESULTS

The principal stress ratio σ_1'/σ_3' versus nominal axial strain responses for the six experiments are shown in Figs. 3(a), 3(b), and 3(c). The five unloading-reloading cycles are visible in all six experiments. The stress-strain traces are characterized by distinct periodic oscillations in stress of similar frequency, amplitude, and pattern in some of the experiments, as inelastic deformations dominant the overall responses. The amplitude of the oscillations increases with confining pressure, being most pronounced in the 1.30 kPa F1 experiment. Also, while the oscillations for all three F1 experiments appear to be of a similar nature, the slip phase of the 1.30 kPa experiment appears to be steeper and to involve greater local instabilities than the other two. This oscillatory behavior is to a large extent attributed to periodic instabilities, which appear to result from buckling and degradation of multiple discrete internal arches

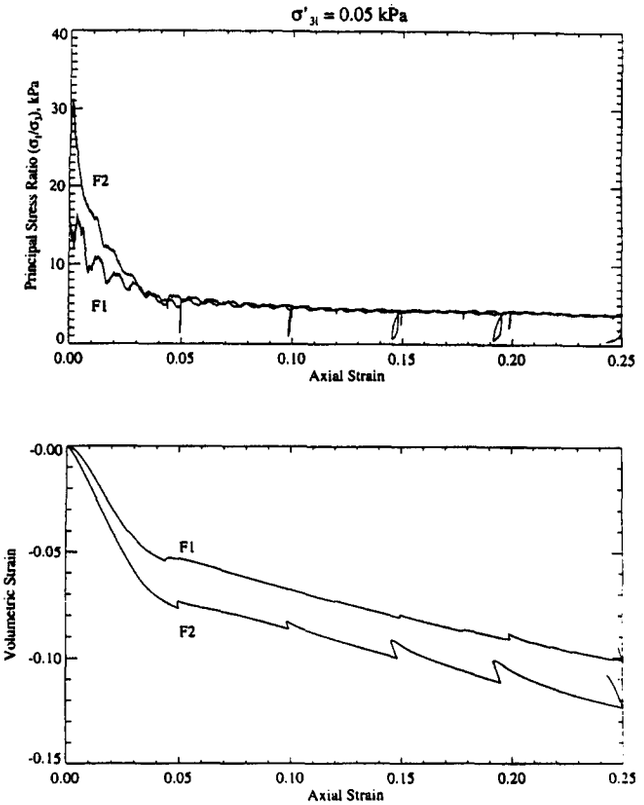

FIG. 3(a). Principal Stress Difference versus Axial Strain Results with Membrane Correction, and Volumetric Strain versus Axial Strain for 0.05 kPa F1 and F2 Experiments

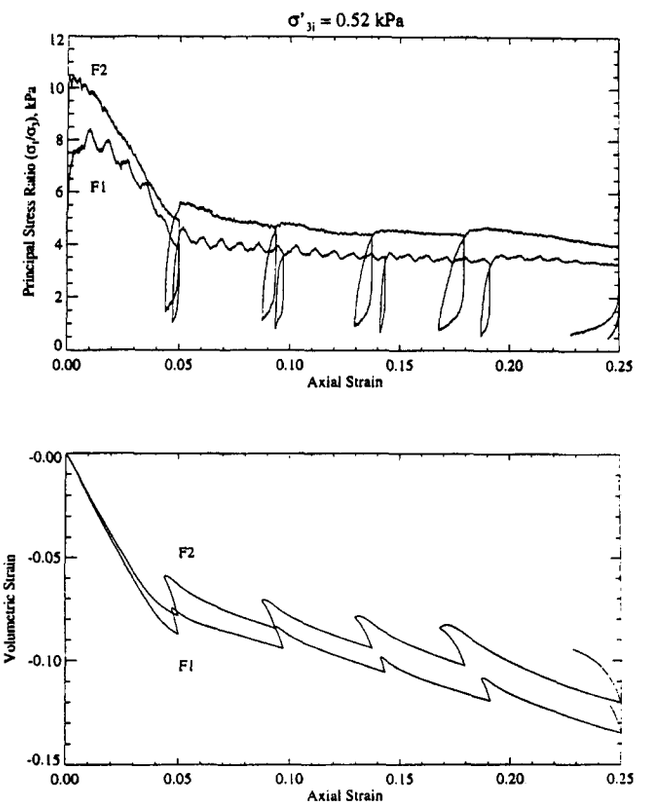

FIG. 3(b). Principal Stress Difference versus Axial Strain Results with Membrane Correction, and Volumetric Strain versus Axial Strain for 0.52 kPa F1 and F2 Experiments

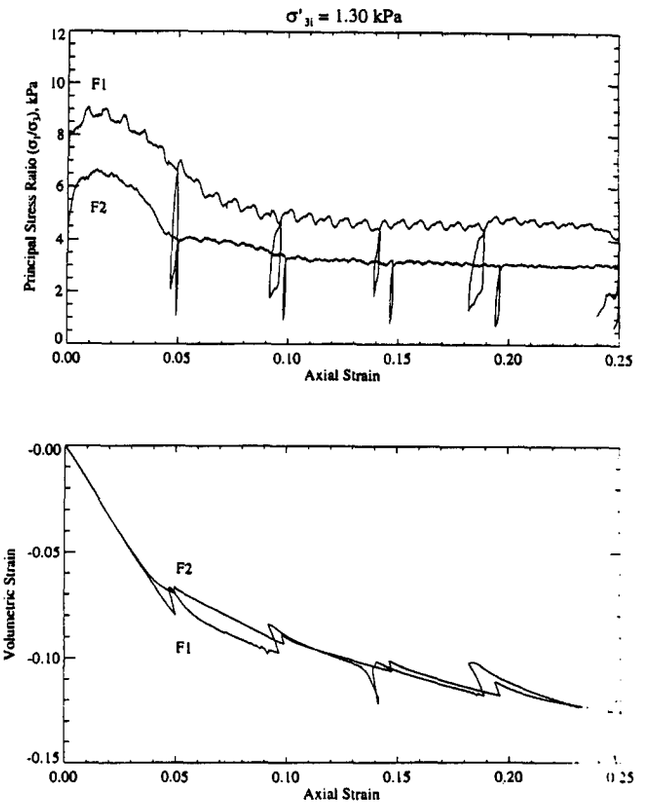

FIG. 3(c). Principal Stress Difference versus Axial Strain Results with Membrane Correction, and Volumetric Strain versus Axial Strain for 1.30 kPa F1 and F2 Experiments

and columnar systems (Jaeger and Nagel 1996; Jaeger et al. 1996). These mechanisms appear to be significantly suppressed in terrestrial (1 gravity) experiments at higher confining stress levels. The unloading-reloading traces in all cases appear to be nearly unaffected by the confining stress level. It is also interesting to observe that the specimens display substantial elastic stiffnesses, with unloading-reloading moduli in the range of 11 to 24 MPa, which do not seem to change even after large axial displacements of 20 to 25% and dilation exceeding 10%. The 0.05 kPa confining pressure experiments show substantial strain softening and loss of stability, and peak resistance or strength at very small strain $(\sigma_1'/\sigma_3')_f = 16.5$ for the F1 test and $(\sigma_1'/\sigma_3')_f = 31.0$ for the F2 test. The responses of the residual strength levels are virtually identical. The stress-strain responses for the 0.52 kPa F1 and F2 experiments show similar initial stiffness to the 0.05 kPa test, and a distinct peak strength of $(\sigma_1'/\sigma_3')_f = 8.5$ for the F1 test and $(\sigma_1'/\sigma_3')_f = 10.5$ for the F2 test. The strain-softening phase is rather ductile in comparison to the 0.05 kPa tests. The response at the residual strength level shows a visibly higher strength for the F2 test. The stress-strain response of the 1.30 kPa experiment shows initial stiffness behavior that is very similar to the lower confinement tests, while the stick-slip pattern is more pronounced. The peak strength in these experiments is $(\sigma_1'/\sigma_3')_f = 9.0$ for the F1 test and $(\sigma_1'/\sigma_3')_f = 6.5$ for the F2 test. The post-peak strain-softening proceeds at a more ductile rate than the 0.52 kPa tests. The residual levels appear to remain quite stable and do not show visible strength reduction, although the F1 residual strength level stays substantially higher than that of the F2 test. The effect of the stretched membrane on the radial confining stress has been included in the analysis. The peak friction angles observed for the six experiments are shown in Table 1.

The observed angles of internal friction are unusually large

TABLE 1. Peak Friction Angle

Test (1)	0.05 kPa (2)	0.52 kPa (3)	1.30 kPa (4)
F1	63.4°	52.1°	53.3°
F2	70.0°	55.8°	47.6°

for a granular soil with initial density in the range of 85% for the F1 tests and 65% for the F2 tests (Bolton 1986). The properties for the same material at the same density, tested at 13.8 and 34.5 kPa, gives angles of 44.1° with standard deviation 0.3. There is a significant difference between the observed strength behavior at low and high stress levels. In the 0.05 kPa test, the peak strength in F1 is visibly lower than that seen in F2, although the initial density for the F1 test is 20% higher than that of the F2 test. The same pattern appears for the two (F1 and F2) 0.52 kPa tests, while the behavior of the 1.30 kPa tests seems consistent with theory. It appears that the relatively higher degree of mobilized resistance in the low confining stress experiments is a result of substantially different deformation mechanisms within the granular fabric, where more work-intensive modes of deformation perhaps involving extensive rotations and sliding occur rather than simple sliding, thus absorbing more of the externally provided energy. The high friction angles can also be attributed to overconsolidation effects, similar to those observed in cohesive soils, which have also been discussed by Lade and Prabucki (1995). The Young's moduli observed in the unloading and reloading traces of the six experiments are as follows: (a) 0.05 kPa tests: 11.8 to 20.0 MPa; (b) 0.52 kPa tests: 16.9 to 21.2 MPa; and (c) 1.30 kPa tests: 17.0 to 23.7 MPa. The postpeak residual strengths and near constant-volume (critical state) friction angles are higher (35–37°) than those observed in terrestrial laboratories, which are typically in the range of 32 to 34° for quartz sand (Bolton 1986).

Figs. 3(a), 3(b), and 3(c) also show volumetric strain versus axial strain response diagrams for the six experiments. The initial responses appear to be very similar for the six experiments with initial dilatancy angles in the range of 30.0 to 31.0°. There appears to be a significant departure from the initial and nearly linear volumetric expansion at the 4 to 5% axial strain level, where the rate of expansion seems to be reduced by a factor of almost five, resulting in an average dilatancy angle of 6 to 6.5°, which remains almost constant to the end of the experiments. None of the specimens displayed evidence of major shear-band formation or other forms of localized deformation. The volumetric changes were generally uniform, with extensive but diffuse bulging at large axial strain levels. The unloading-reloading response traces of the 0.05 and 0.52 kPa experiments show pronounced dilatancy during both unloading and reloading stages although the responses also indicate significant elastic behavior, which is seen to a far lesser extent in experiments conducted at high confining stress levels. The volumetric unloading-reloading cycles show very similar stiffness modulus behavior and insignificant relationship between either deformation level or effective confining pressure. In all three experiments the initial stiffness moduli are similar to the unloading-reloading moduli. Based on the difference in the volumetric responses at axial strains before and after 4%, it appears that very different deformation mechanisms are involved. Secondary sets of shear bands form at regular spacings, where dilation in these bands results in additional increases in volumetric strain rather than leveling of the volumetric versus axial strain traces. This may explain the relatively high residual strength levels.

In order to study the internal consistency of the experimental findings and boundary (including membrane) effects, and to enhance the understanding of overall specimen behavior, nonlinear three-dimensional (3D) finite-element analyses of the specimen-membrane-end-platen system were conducted. Fig. 4 shows a composite diagram of the experimental and finite-element analyses of the three load-displacement responses, where the membrane effect is included and not corrected, as shown in Figs. 3(a), 3(b), and 3(c). The details of the analyses and the constitutive model and parameters used are described by Jeremic (1997). The correspondence between the experiments and the analyses, using a consistent set of material parameters, which were obtained from separate experiments, show that the findings are reasonable and show internal consistency.

Following the experiments the specimens were stabilized by epoxy impregnation and the internal features were studied using X-ray computed tomography techniques provided by the Non-Destructive Testing and Evaluation facility of Los Alamos National Laboratory and the Kennedy Space Center Computed Tomography System. Data from each specimen consists of cross-axial slices at 1 mm vertical spacing. The slices are used to construct 3D volumetric images of the specimen, and inner features may then be examined by exposing internal planes. In the images shown in Figs. 5 and 6, darker colored pixels represent areas of lower densities, generally where the material has dilated during shearing. Circular shear cones are seen extending at large angles from each end of the specimens, though the cone on the stationary end platen is more clearly developed. A large number of inclined, radial

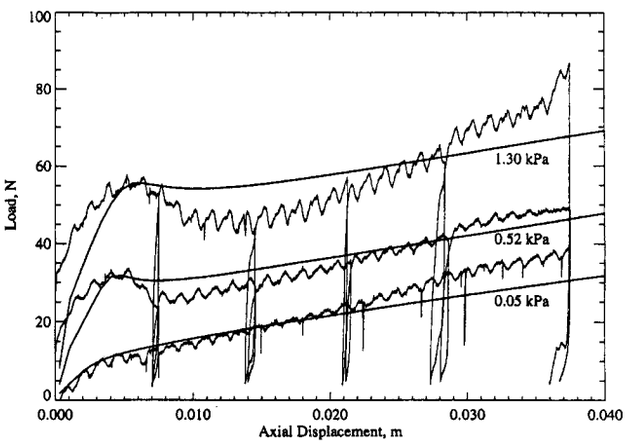

FIG. 4. Finite-Element Analysis Predictions of Load-Displacement Responses for Three Experiments (0.05, 0.52, and 1.30 kPa Confining Stress). Membrane Effect Included. Wide Lines Show Prediction and Jagged Response Traces Show Experiment Responses

FIG. 5. Vertical Slice Produced by X-Ray Computed Tomography and Visualization of Epoxy-Impregnated Specimen

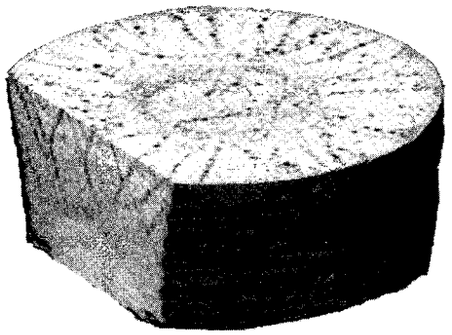

FIG. 6. Vertical and Horizontal Slice Produced by X-ray Computed Tomography and Visualization of Epoxy-Impregnated Specimen

discrete bands of lower density, similar in shape to turbine blades mounted on a central hub, extend outward from the boundary of the cones. The cones are clearly defined by the specimen-end-platen interface friction and the restraint posed by the stretched latex membrane in the external contact region.

CONCLUSIONS

The six experiments that were conducted at low effective confining stresses in microgravity show very high peak strength friction angles in the range of 47.6 to 70.0°, which are mainly due to overconsolidation and grain interlocking effects. It was observed that the residual strength levels in all six cases were in the same range as that observed at higher confinement levels. While the specimens still dilate at high strain levels, the low dilatancy angles at this stage (3°) do not account for this phenomenon. All specimens display substantial initial stiffnesses and elastic moduli during unloading and reloading events, which are nearly an order of magnitude higher than conventional theories predict.

ACKNOWLEDGMENTS

The writers gratefully acknowledge support provided by NASA, Marshall Flight Center. Contract NAS8-38779 to the University of Colorado, Boulder, Colo. This material is also based in part upon work supported under a National Science Foundation Graduate Fellowship. The writers also wish to acknowledge advice and assistance at various stages of this project from Alfredo Baeza, Robert Habbit, George Alder, and Todd Adelman, of Sandia National Laboratories, Albuquerque, N.M.; Martin Jones and David Stupin of Los Alamos National Laboratory; Peter Engel of the Kennedy Space Center Computed Tomography System; and Buddy Guynes, Tom Stinson, Jerry Shelby, John Oddo, Ron Cantrell, Ron Porter, and Joel Kearns of NASA Marshall Space Flight Center, Huntsville, Ala.

APPENDIX. REFERENCES

Bolton, M. D. (1986). "The strength and dilatancy of sands." *Géotechnique*, London, U.K., 36(1), 65–78.

Costes, N. C., and Sture, S. (1981). "The potential for soil dynamics research in space." *Proc., Int. Conf. on Recent Advances in Geotechnical Earthquake Engrg. and Soil Dyn.*, Vol. 3, University of Missouri Press, St. Louis, Mo., 929–959.

Jaeger, H. M., and Nagel, S. R. (1996). "Physics of the granular state." *J. Sci.*, 255, 1523–1531.

Jaeger, H. M., and Nagel, S. R. (1997). "Dynamics of granular material." *Am. Sci.*, 85, 540–545.

Jaeger, H. M., Nagel, S. R., and Behringer, R. P. (1996). "The physics of granular materials." *Phys. Today*, April, 32–38.

Jeremic, B. (1997). "Finite deformation hyperelasto-plasticity of geomaterials," PhD dissertation, University of Colorado, Boulder, Colo.

Lade, P. V., and Prabucki, M. J. (1995). "Softening and preshearing effects in sand." *J. Soils and Found.*, 35(4), 93–104.

Scholz, C. H. (1990). *Mechanics of earthquakes and faulting*. Cambridge University Press, Cambridge, U.K.

Sture, S., Runesson, K., and Macari-Pasqualino, E. J. (1988). "Analysis and calibration of a three-invariant plasticity model for granular materials." *J. Ingenieur-Archiv*, 59, 253–266.